Interfacial Charge States in Graphene on SiC Studied by Noncontact Scanning Nonlinear Dielectric Potentiometry

Kohei Yamasue,* Hirokazu Fukidome, Kazutoshi Funakubo, Maki Suemitsu, and Yasuo Cho
Research Institute of Electrical Communication, Tohoku University, 2-1-1 Katahira, Aoba, Sendai 980-8577, Japan
(Received 23 December 2014; published 4 June 2015)

We investigate pristine and hydrogen-intercalated graphene synthesized on a 4*H*-SiC(0001) substrate by using noncontact scanning nonlinear dielectric potentiometry (NC-SNDP). Permanent dipole moments are detected at the pristine graphene-SiC interface. These originate from the covalent bonds of carbon atoms of the so-called buffer layer to the substrate. Hydrogen intercalation at the interface eliminates these covalent bonds and the original quasi-(6×6) corrugation, which indicates the conversion of the buffer layer into a second graphene layer by the termination of Si bonds at the interface. NC-SNDP images suggest that a certain portion of the Si dangling bonds remains even after hydrogen intercalation. These bonds are thought to act as charged impurities reducing the carrier mobility in hydrogen-intercalated graphene on SiC.

DOI: 10.1103/PhysRevLett.114.226103 PACS numbers: 68.65.Pq, 61.48.Gh, 72.80.Vp, 73.22.Pr

Graphene is a carbon-based two-dimensional crystalline particularly promising for high frequency electronic device applications owing to its extremely high achievable carrier mobility [1–3]. Among the various synthesis methods [1,4–6], the thermal decomposition of a SiC surface in an Ar atmosphere has enabled the direct formation of large graphene sheets on SiC wafers. Since this method eliminates the need for the transfer of synthesized graphene sheets onto another substrate, it will likely become an important technological base for the mass production of graphene-based integrated electronic devices [6].

However, the electronic properties of graphene on SiC are very different from those of a free-standing monolayer of graphene [7]. Monolayer graphene (MLG) on SiC is *n* doped and its Fermi level position is higher than the Dirac point [7–9]. In addition, its carrier mobility has a strong temperature dependence [10,11] and is typically limited to about 900 $\mathrm{cm}^2/\mathrm{V\,s}$ at room temperature [6,10]. This is much lower than the mobility for mechanically exfoliated MLG [1,12]. These differences from freestanding graphene have been attributed to the presence of the buffer layer, or $(6\sqrt{3} \times 6\sqrt{3})$-$R30°$ reconstructed interface, between MLG and the SiC substrate [13,14]. This buffer layer has a graphenelike honeycomb structure, with some of the carbon atoms covalently bonded to the Si atoms on the substrate [13–17]. Because of the dominant phonon scattering from the substrate, there is a strong temperature dependence of the mobility which is greatly reduced at room temperature [10,11].

The hydrogen-intercalation method is key to decoupling the buffer layer from the substrate and increasing the mobility [18]. Breaking the covalent bonds and terminating the Si atoms at the interface with atomic hydrogen bring the graphene layers into a quasifreestanding state. However, even after hydrogen intercalation, the carrier mobility remains significantly lower than that for ideal freestanding graphene [19–21]. The carrier mobility shows no strong temperature dependence and has hitherto been limited to about 3000 $\mathrm{cm}^2/\mathrm{V\,s}$ [19,20]. By optimizing the annealing temperature, Tanabe *et al.* have achieved 4000 $\mathrm{cm}^2/\mathrm{V\,s}$ recently [21]. The limited mobility has been attributed to scattering by charged impurities at the interface [20–22]. It is therefore important to determine the charge states at the interface in order to understand and improve the electronic transport properties by hydrogen intercalation of graphene on SiC [23]. In particular, Si dangling bonds at the interface have attracted interest, since they supply electrons to the graphene layer and act as charged impurities in the system [21–23].

In this study, noncontact scanning nonlinear dielectric potentiometry (NC-SNDP) [24] is utilized to investigate the interfacial charge state in pristine and hydrogen-intercalated graphene on 4*H*-SiC(0001) substrates. NC-SNDP is a scanning probe microscopy method that is selectively sensitive to potentials induced by spontaneous polarization (or permanent dipole moments) on surfaces and interfaces. This method can detect a nonlinear variation in the tip-sample capacitance (ΔC_{ts}) under an external electric field using a gigahertz-range *LC* oscillator [25]. Among the higher-order nonlinear effects caused by the high electric field localized under the tip, second- and third-order effects are employed [26] to acquire, respectively, polarization-induced potentials and topographic features. The second-order signal is null balanced by applying a dc potential effectively canceling spontaneous polarization [24]. The dc potential is then approximately equivalent to the polarization-induced potential under the tip. The third-order signal is utilized for keeping the tip-sample distance and imaging topography, since it monotonically and rapidly increases as the tip gets closer to the surface [26]. ΔC_{ts} is measured by demodulating the frequency shift of the oscillator (Δf), since the *LC* tank circuit is

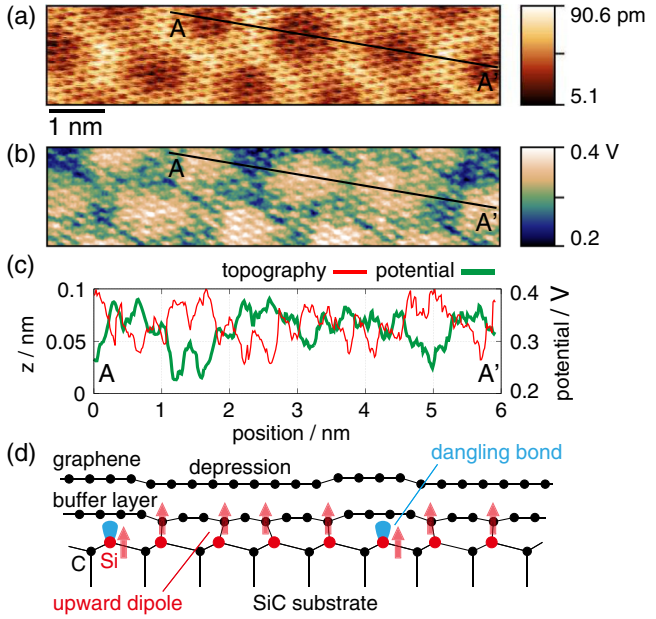

FIG. 1 (color online). Simultaneous NC-SNDP images of monolayer graphene on a 4*H*-SiC(0001) substrate. (a) Topography, (b) potential, (c) profiles along the line from A to A' in (a) and (b), respectively. (d) Cross-sectional schematic of monolayer graphene on a SiC(0001) substrate.

electrically coupled in parallel with the tip-sample capacitance. By modulating the electric field, the different order effects can be simultaneously detected, because they generate different order higher harmonics in Δf. Kelvin probe force microscopy (KPFM) can determine potentials through the measurement of the electrostatic tip-sample interaction force [27], which differs from NC-SNDP in that it does not distinguish the contributions from the contact potential difference, fixed monopole charges, and spontaneous polarization. Details of NC-SNDP have been described in Ref. [24] (or see a brief review in Ref. [28]).

Here, MLG was synthesized on an n-type diced 4*H*-SiC(0001) wafer by annealing it in Ar under atmospheric pressure [6]. The substrate was almost entirely covered with MLG. The NC-SNDP measurements were performed in an ultrahigh vacuum with a base pressure of about 5×10^{-11} Torr at room temperature. A Pt-Ir tip was mounted on an LC oscillator with an oscillation frequency of about 1.7 GHz. The apex of the tip was cleaned by an Ar^+ beam before the measurement. The data were acquired using a Dulcinea Control System controlled by the software WSXM (Nanotech Electrónica, S. L.) [31]. The images were treated by the software GWYDDION [32].

Figure 1 shows NC-SNDP images of pristine MLG on a 4*H*-SiC(0001) substrate. The modulation voltage was 1.5 V_{pp} at 25 kHz. The topographic image [Fig. 1(a)] reveals a honeycomb structure on which a larger honeycomb-shaped corrugation is superimposed. The same features have been observed by scanning tunneling microscopy (STM) [33]. Since the smaller hexagons have a side length of 0.14 nm, which roughly corresponds to the C-C bond length in graphene (0.142 nm), NC-SNDP can resolve a graphene layer at the atomic scale. The corrugations exhibit a so-called quasi-(6×6) periodicity arising from the underlying $6\sqrt{3} \times 6\sqrt{3}$-$R30°$ reconstructed interface [33]. The potential image in Fig. 1(b) displays a positive spatial-averaged potential of 0.32 V. NC-SNDP is sensitive to dipole-induced potentials in the z (out-of-plane) direction [24], which suggests the presence of permanent upward (outward pointing normal to surface) dipoles. The dipoles could occur in either the topmost graphene layer or the SiC substrate or at the interface. The first possibility can be ruled out, because each C atom in graphene has a spatially symmetric charge distribution owing to its sp^2 configuration [13,15,33]. Thus, no significant permanent dipole is observed. The second possibility is related to spontaneous polarization of the 4*H*-SiC substrate along the c axis. However, this is unlikely to contribute to ΔC_{ts} because of the high density of surface states. Since the Fermi level will be pinned [14,19], an electric field from the tip does not penetrate the substrate appreciably [34]. This also indicates that the variation in capacitance associated with the depletion layer in the SiC substrate, which can induce ΔC_{ts}, is negligible, whereas it can be prominent for an insulating surface.

The detected positive potentials are therefore attributed to dipoles at the interface. As illustrated in Fig. 1(d), the depressions of the quasi-(6×6) corrugation have C atoms that are covalently bonded to Si atoms on the SiC subsurface [13–17]. Each of these C atoms has an asymmetric charge distribution around it, forming upward dipoles. This is because, as a result of the covalent bonding, instead of π bonds with a symmetric electron distribution in the z direction, a negatively charged σ bond is newly formed toward a Si atom beneath the C atom. A permanent electric dipole moment in the z direction is then produced by a positively charged atomic nucleus and the negatively charged σ bond below it. The σ bond is off center with respect to the C nucleus and connected to a Si atom below the C atom. Note that sp^2 to sp^3 rehybridization should be taken into account here. If the rehybridization is ideal, the covalently bonded C atom eventually has sp^3 symmetry with no permanent dipole. However, our experimental results, which reveal the presence of upward dipoles, suggest that the rehybridization is not perfect, as predicted by previous first-principles calculations [16,35]. Although sp^3 rehybridization occurs, contributing to interface stability, the pyramidalization angles about the C atoms end up being smaller than the ideal angle for the sp^3 configuration [35]. The profiles in Fig. 2(c) show that the measured potentials remained positive but lower in the ridges of the quasi-(6×6) corrugation. This indicates that the upward dipole moments decreased owing to the lower density of C atoms covalently bonded to the substrate. The presence of this dipole layer oriented toward the vacuum would

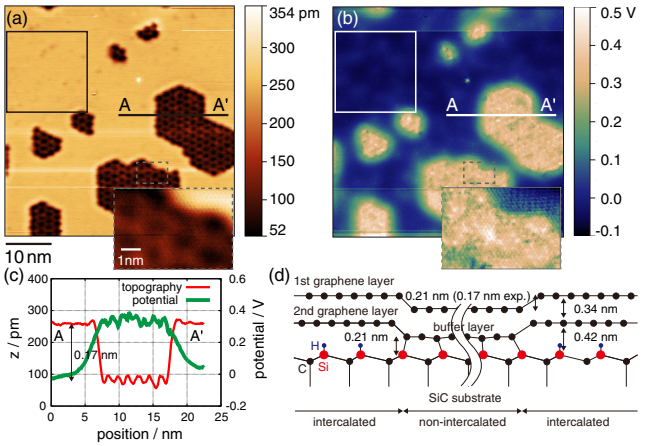

FIG. 2 (color online). Simultaneous NC-SNDP images of partially hydrogen-intercalated graphene on a 4*H*-SiC(0001) substrate. (a) Topography, (b) potential, (c) profiles along the line from A to A' in (a) and (b). (d) Schematic of the height difference between hydrogen-intercalated and non-intercalated areas. The distances indicated in (d) are adopted from Ref. [36]. 0.17 nm is the measured height difference between hydrogen-intercalated and non-intercalated areas. The solid boxed areas in (a) and (b) are magnified in Fig. 3. The insets of (a) and (b) are higher resolution images of the gray dashed rectangles in (a) and (b). The double wavy line in (d) indicates the omission of repetitive quasi-(6×6) features (not drawn) within non-intercalated areas.

decrease the work function of the buffer layer on SiC(0001) relative to that of a pristine SiC(0001) surface [14].

Note that the tip height plays a minor role in this potential measurement. This is because the (6×6) corrugation in the topographic image is dominated by geometric effects rather than electronic structures [15]. During a lateral scan, no significant change occurs in the distance between the tip and the buffer layer, as long as the tip-surface distance is kept constant by the main z feedback. The measured potentials are modulated by variations in electronic structure or charge density at the atomic scale, leading to hexagonal features aligned with the honeycomb structure of the topmost graphene layer (see Ref. [28] for the details of the correlation between the topography and potential images).

Hydrogen intercalation dramatically changes both the topographic features and the potential distribution. Figures 2(a) and 2(b) show simultaneous NC-SNDP images of hydrogen-intercalated graphene on an n-type 4*H*-SiC(0001) substrate. The sample was prepared by annealing MLG synthesized on a 4*H*-SiC(0001) substrate at 800 °C for 10 min in argon-diluted hydrogen gas at atmospheric pressure. The samples were heated at 600 °C for 30 min in an ultrahigh vacuum prior to measurements to eliminate any adsorbates on the surface. The desorption of intercalated hydrogen has been reported to be insignificant below 650 °C [37]. The modulation voltage was 1.0 V_{pp} at 25 kHz. The observed area was 50 nm^2, which is much larger than that of Fig. 1. In the topographic image, we find that a large part of the surface was covered with newly emerged flat areas [as seen, for example, in the solid boxed area in Fig. 2(a)]. The emergence of such flat areas in a partly hydrogen-intercalated sample has also been reported in studies using STM [37–39]. The averaged potential was notably reduced to an almost neutral level, as shown in Fig. 2(b). We also see darker patches recessed from the flat areas. These patches share the polygonal shape reported previously for quasifreestanding MLG [37], whereas the present case is quasifreestanding bilayer graphene (BLG) as discussed below. Within these polygonal patches, the quasi-(6×6) corrugation is observed, as shown in the insets of Figs. 2(a) and 2(b). The averaged potentials remained at 0.33 V in these areas, which agrees with that for pristine MLG, shown in Fig. 1(b). Thus, it appears that these polygonal corrugated areas were not hydrogen intercalated. The fact that the flat areas coexisted with the quasi-(6×6) surface suggests that graphene was partially hydrogen intercalated in this sample. Figure 2(c) shows topographic and potential profiles along the line from A to A'. As shown in Fig. 2(c), the flat areas were 0.17 nm higher than the corrugated areas in the z direction. This height difference is comparable to the distance from the buffer layer to the substrate (0.21 nm in Ref. [36]) and the distance from the hydrogen-intercalated buffer layer to the substrate (0.42 nm) [36]. This implies that the flat areas were BLG arising from hydrogen intercalation. The situation is illustrated in Fig. 2(d). Since Si-C covalent bonds were broken and Si atoms at the interface were terminated by hydrogen atoms, the buffer layer was relaxed and then converted into a second graphene layer [18]. The large corrugations were reduced, since graphene layers were decoupled from the substrate by hydrogen intercalation. In the flat areas, the average potential decreased to almost −0.03 V. Since NC-SNDP is sensitive to the potential induced by electric dipoles or an asymmetric charge distribution, the dipole moments at the interface were reduced by hydrogen intercalation. This implies that the covalent bonds were eliminated and a second layer graphene was formed along with a symmetric charge distribution. The hydrogen-terminated Si atoms took on an sp^3 configuration and thus no significant dipole moments were detected, similar to the case of hydrogen-adsorbed Si adatoms on a Si(111)-(7×7) surface [40]. Note that the second layer may screen the interface from electric fields from the tip to some extent and thus apparently reduce the measured potentials. However, the screening effect cannot explain the drastic potential decrease from 0.33 V to −0.03 V shown here. This was confirmed by measuring BLG on the buffer layer, where the average potential was only 0.14 V lower than that on MLG (see Ref. [28] for the details).

It is interesting to note the polygonal shape of the quasi-(6×6) areas. This characteristic shape implies that each quasi-(6×6) cell is a unit for the progress of hydrogen intercalation. The reaction is initiated at some preferential

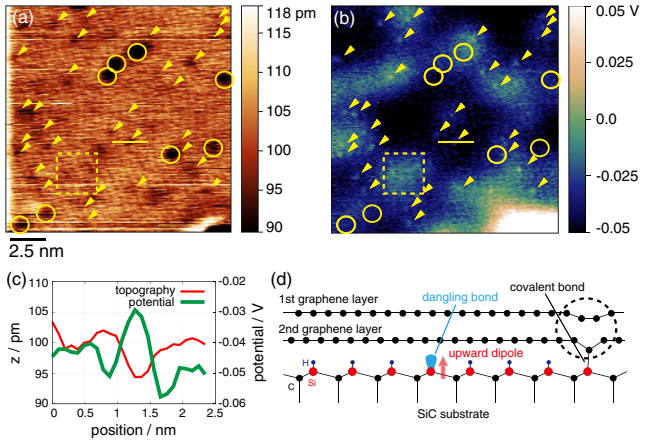

FIG. 3 (color online). Magnified NC-SNDP images of the square areas in Figs. 2(a) and 2(b). (a) Topography, (b) potential. In (b), small bright spots are indicated by yellow arrowheads. The corresponding positions are also shown by arrowheads in (a). Yellow circles in (a) indicate distinct depressions in the topography. (c) A typical example of topographic and potential profiles in a spot (Profiles along the yellow solid lines in (a) and (b)). (d) Schematic model of the imaged hydrogen-intercalated interface.

sites such as defects in the first layer graphene. Once the termination of Si bonds with hydrogen begins on a given cell, that cell is readily decoupled from the substrate. This is because the cell now has fewer covalent bonds, resulting in a weaker coupling of the buffer layer to the substrate on that cell. This implies that cells neighboring the intercalated cell become new preferential reaction sites in the next step. Then, the resulting intercalated BLG areas extend over the interface through a cell-by-cell reaction, and finally contact one another, thus completing the formation of a homogeneous BLG.

Figures 3(a) and 3(b) show magnified images of the solid boxed area in Figs. 2(a) and 2(b), respectively. The contrast of these images is enhanced to highlight small topographic features and potential variations. The magnified area appears to be topographically rather flat; however, in the potential image, one can find many small bright spots with slightly higher potentials as indicated by yellow arrowheads in Fig. 3(b). The profile for a typical spot is shown in Fig. 3(c). The potentials on the spots are ~20 mV higher than those on the homogeneous area. The radii of these spots range from 0.2 nm to 0.3 nm, which corresponds to an atomic scale. Although, corresponding to each of these spots, small depressions are found in the topographic image, their depth are as shallow as ~10 pm. This implies that the observed spots arise from the charge states at the interface rather than charged particles or adsorbates on the surface. Since NC-SNDP is sensitive to atomic dipoles [40–42], the confined potential contrast can be said to be due to the atomic charges at the interface. Possible candidates for the atomic charges are defects on the SiC substrate or the second graphene layer, and Si atoms with dangling bonds. A core-level photoelectron spectroscopy study has recently suggested that a significant number of Si dangling bonds persist at the hydrogen-intercalated interface [20–22]. Since Si dangling bonds supply electrons to the graphene layer, these Si atoms are positively charged on the vacuum side, similar to the Si adatoms on a Si(111)-(7 × 7) surface [41]. As illustrated in Fig. 3(d), this results in the formation of permanent upward dipoles at the interface, which is consistent with the direction of the dipoles at the spots, determined by NC-SNDP. The density of these spots is estimated to be roughly 1×10^{13} cm^{-2}, which is, surprisingly, comparable to the estimated density of charged impurities in hydrogen-intercalated graphene on SiC(0001) reported by Tanabe *et al.* [21]. We therefore conclude that the Si dangling bonds at the interface were visualized by NC-SNDP. Similar results have recently been obtained by Murata *et al.* using STM [23]. However, the previous study in Ref. [43] indicates that the atomic spots were truly visualized through the measurement of ΔC_{ts}, while NC-SNDP was operated in a tunneling regime.

There are also some distinct depressions in the flat area, denoted by yellow circles in Fig. 3(a). The typical depth is 20 to 30 pm, and the width is 2 nm in the topographic image. Since the width is comparable to the period of the quasi-(6 × 6) structure, each depression may correspond to a very small polygonal-shaped area with covalent bonds at the interface. In contrast to the spots, the positions of the depressions do not correlate with those of higher-potential areas. This suggests that there are no significant atomic-scale permanent dipoles at the interface. The smaller dipole moments may be induced by larger pyramidalization angles about the few covalent bonds persisting at the interface, as illustrated in the dashed circle in Fig. 3(d). The much smaller depth in topography compared to those of the other large polygonal-shaped areas may be due to a geometric limitation to keep the continuity of the first graphene layer over these depressions. Note that other fluctuations are observed in the potential image. A typical example is shown in the dashed square in Fig. 3(b). Areas with slightly higher potentials extend over several nanometers but do not seem to correlate with any of the abovementioned topographic features such as the spots and depressions in Fig. 3(a). Although these fluctuations could be related to a spatial variation of charge density on the graphene layers, their cause has not yet been identified.

In summary, NC-SNDP imaging suggested the presence of permanent dipole moments at the interface of pristine MLG on a 4*H*-SiC(0001) substrate. These dipoles are formed by C atoms covalently bonded to the substrate. Upon hydrogen intercalation, the quasi-(6 × 6) corrugations disappear, the topmost graphene layer is relaxed, assuming an extremely flat shape, and the dipole moments vanish. These results indicate that the buffer layer becomes a second graphene layer and the Si dangling bonds are terminated by

hydrogen, as expected. NC-SNDP images also suggest that some of the Si dangling bonds remain even after hydrogen intercalation. These bonds are believed to act as charged impurities significantly affecting electronic transport in hydrogen-intercalated graphene on SiC [20–23].

We thank Dr. Yuya Murata and Dr. Stefan Heun of NEST, Istituto Nanoscienze, CNR, and Scuola Normale Superiore for fruitful discussion. We also thank Masao Uno of Murata Manufacturing Co. Ltd. and Toshihiko Iwai of Research Institute of Electrical Communication, Tohoku University, for providing support in the development of high-sensitivity probes. This work is supported in part by a Grant-in-Aid for Scientific Research (23226008, 15K04673) from Japan Society for the Promotion of Science.

*yamasue@riec.tohoku.ac.jp

[1] K. S. Novoselov, A. K. Geim, S. V. Morozov, D. Jiang, Y. Zhang, S. V. Dubonos, I. V. Grigorieva, and A. A. Firsov, Science **306**, 666 (2004).
[2] C. Berger, Z. Song, Z. Xuebin Li, X. Wu, N. Brown, C. Naud, D. Mayou, T. Li, J. Hass, A. N. Marchenkov, E. H. Conrad, P. N. First, and W. A. de Heer, Science **312**, 1191 (2006).
[3] S. V. Morozov, K. S. Novoselov, M. I. Katsnelson, F. Schedin, D. C. Elias, J. A. Jaszczak, and A. K. Geim, Phys. Rev. Lett. **100**, 016602 (2008).
[4] C. Berger, Z. Song, T. Li, X. Li, A. Y. Ogbazghi, R. Feng, Z. Dai, A. N. Marchenkov, E. H. Conrad, P. N. First, and W. A. de Heer, J. Phys. Chem. B **108**, 19912 (2004).
[5] P. W. Sutter, J.-I. Flege, and E. A. Sutter, Nat. Mater. **7**, 406 (2008).
[6] K. V. Emtsev, A. Bostwick, K. Horn, J. Jobst, G. L. Kellogg, L. Ley, J. L. McChesney, T. Ohta, S. A. Reshanov, J. Rohrl, E. Rotenberg, A. K. Schmid, D. Waldmann, H. B. Weber, and T. Seyller, Nat. Mater. **8**, 203 (2009).
[7] T. Ohta, A. Bostwick, T. Seyller, K. Horn, and E. Rotenberg, Science **313**, 951 (2006).
[8] S. Y. Zhou, G. H. Gweon, A. V. Fedorov, P. N. First, W. A. de Heer, D. H. Lee, F. Guinea, A. H. Castro Neto, and A. Lanzara, Nat. Mater. **6**, 770 (2007).
[9] C. Riedl, A. A. Zakharov, and U. Starke, Appl. Phys. Lett. **93**, 033106 (2008).
[10] J. Jobst, D. Waldmann, F. Speck, R. Hirner, D. K. Maude, T. Seyller, and H. B. Weber, Phys. Rev. B **81**, 195434 (2010).
[11] S. Tanabe, Y. Sekine, H. Kageshima, M. Nagase, and H. Hibino, Phys. Rev. B **84**, 115458 (2011).
[12] K. S. Novoselov, Z. Jiang, Y. Zhang, S. V. Morozov, H. L. Stormer, U. Zeitler, J. C. Maan, G. S. Boebinger, P. Kim, and A. K. Geim, Science **315**, 1379 (2007).
[13] F. Varchon, R. Feng, J. Hass, X. Li, B. N. Nguyen, C. Naud, P. Mallet, J.-Y. Veuillen, C. Berger, E. H. Conrad, and L. Magaud, Phys. Rev. Lett. **99**, 126805 (2007).
[14] A. Mattausch and O. Pankratov, Phys. Rev. Lett. **99**, 076802 (2007).
[15] F. Varchon, P. Mallet, J.-Y. Veuillen, and L. Magaud, Phys. Rev. B **77**, 235412 (2008).
[16] S. Kim, J. Ihm, H. J. Choi, and Y.-W. Son, Phys. Rev. Lett. **100**, 176802 (2008).
[17] K. V. Emtsev, F. Speck, T. Seyller, L. Ley, and J. D. Riley, Phys. Rev. B **77**, 155303 (2008).
[18] C. Riedl, C. Coletti, T. Iwasaki, A. A. Zakharov, and U. Starke, Phys. Rev. Lett. **103**, 246804 (2009).
[19] F. Speck, J. Jobst, F. Fromm, M. Ostler, D. Waldmann, M. Hundhausen, H. B. Weber, and T. Seyller, Appl. Phys. Lett. **99**, 122106 (2011).
[20] S. Tanabe, M. Takamura, Y. Harada, H. Kageshima, and H. Hibino, Appl. Phys. Express **5**, 125101 (2012).
[21] S. Tanabe, M. Takamura, Y. Harada, H. Kageshima, and H. Hibino, Jpn. J. Appl. Phys. **53**, 04EN01 (2014).
[22] F. Maeda, S. Tanabe, S. Isobe, and H. Hibino, Phys. Rev. B **88**, 085422 (2013).
[23] Y. Murata, T. Mashoff, M. Takamura, S. Tanabe, H. Hibino, F. Beltram, and S. Heun, Appl. Phys. Lett. **105**, 221604 (2014).
[24] K. Yamasue and Y. Cho (to be published).
[25] Y. Cho, A. Kirihara, and T. Saeki, Rev. Sci. Instrum. **67**, 2297 (1996).
[26] K. Ohara and Y. Cho, Nanotechnology **16**, S54 (2005).
[27] M. Nonnenmacher, M. P. O'Boyle, and H. K. Wickramasinghe, Appl. Phys. Lett. **58**, 2921 (1991).
[28] See Supplemental Material at http://link.aps.org/supplemental/10.1103/PhysRevLett.114.226103 for a brief review on NC-SNDP, the details of the correlation between topographic and potential images, and the details of potentials on pristine BLG, which includes Refs. [29,30].
[29] T. Filleter, K. V. Emtsev, T. Seyller, and R. Bennewitz, Appl. Phys. Lett. **93**, 133117 (2008).
[30] H. Huang, W. Chen, S. Chen, and A. T. S. Wee, ACS Nano **2**, 2513 (2008).
[31] I. Horcas, R. Fernández, J. M. Gómez-Rodríguez, J. Colchero, J. Gómez-Herrero, and A. M. Baro, Rev. Sci. Instrum. **78**, 013705 (2007).
[32] D. Nečas and P. Klapetek, Central Eur. J. Phys. **10**, 181 (2012).
[33] P. Mallet, F. Varchon, C. Naud, L. Magaud, C. Berger, and J.-Y. Veuillen, Phys. Rev. B **76**, 041403 (2007).
[34] M. McEllistrem, G. Haase, D. Chen, and R. J. Hamers, Phys. Rev. Lett. **70**, 2471 (1993).
[35] G. Sclauzero and A. Pasquarello, Phys. Rev. B **85**, 161405 (2012).
[36] J. D. Emery, V. H. Wheeler, J. E. Johns, M. E. McBriarty, B. Detlefs, M. C. Hersam, D. Kurt Gaskill, and M. J. Bedzyk, Appl. Phys. Lett. **105**, 161602 (2014).
[37] S. Forti, K. V. Emtsev, C. Coletti, A. A. Zakharov, C. Riedl, and U. Starke, Phys. Rev. B **84**, 125449 (2011).
[38] S. Watcharinyanon, C. Virojanadara, J. Osiecki, A. Zakharov, R. Yakimova, R. Uhrberg, and L. Johansson, Surf. Sci. **605**, 1662 (2011).
[39] S. Goler, C. Coletti, V. Piazza, P. Pingue, F. Colangelo, V. Pellegrini, K. V. Emtsev, S. Forti, U. Starke, F. Beltram, and S. Heun, Carbon **51**, 249 (2013).
[40] D. Mizuno, K. Yamasue, and Y. Cho, Appl. Phys. Lett. **103**, 101601 (2013).
[41] Y. Cho and R. Hirose, Phys. Rev. Lett. **99**, 186101 (2007).
[42] M. Suzuki, K. Yamasue, M. Abe, Y. Sugimoto, and Y. Cho, Appl. Phys. Lett. **105**, 101603 (2014).
[43] K. Yamasue and Y. Cho, J. Appl. Phys. **113**, 014307 (2013).